Analyst

Accepted Manuscript

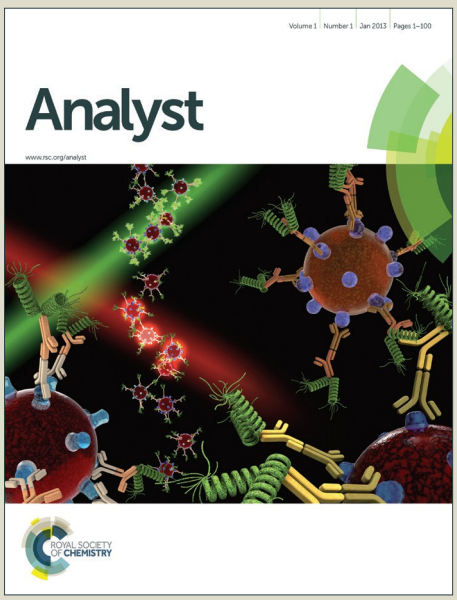

ROYAL SOCIETY OF CHEMISTRY

www.rsc.org/analyst

ZnO oxide films for ultrasensitive, rapid, and label-free detection of Neopterin by surface–enhanced Raman spectroscopy

Agnieszka Kamińska[a,*], Aneta Aniela Kowalska[a], Dmytro Snigurenko[b], Elżbieta Guziewicz[b], Janusz Lewiński[a], and Jacek Waluk[a]

[a] Institute of Physical Chemistry, Polish Academy of Sciences, Kasprzaka 44/52, 01-224 Warsaw, Poland

[b] Institute of Physics, Polish Academy of Sciences, Al. Lotników 32/46, 02-668 Warsaw, Poland

Abstract

An efficient and low-cost surface-enhanced Raman scattering (SERS) substrates based on Au coated zinc oxide layers for the detection of neopterin were prepared. These substrates presented high sensitivity to *p*-mercaptobenzoic acid (*p*-MBA) at a low concentration of 10^{-9} M and the enhancement factor of over 10^7 was achieved. The uniform density of SERS–active "hot-spots" on a Si/ZnO/Au surface results in high reproducibility towards detecting *p*-MBA at 50 different, randomly selected positions on a single substrate (RSD = 9%) and on six different SERS substrates prepared under identical conditions (RSD = 11%). These SERS substrates show good performance in the detection of neopterin, a biologically important molecule whose concentration levels reflect the stage of activation of the cellular immune system, which is of value in studies of pathogenesis and progression of various diseases. The detection limit is found to be as low as 1.4 nmol/L in blood plasma, which is comparable to that of classic ELISA methods. The average relative standard deviation (RSD) of the proposed method is less than 10%. Moreover, this label–free strategy of detection gives exact results over a large range, reflecting clinically relevant neopterin concentrations in body fluids. The detection and quantification of neopterin levels in blood or urine might be useful

in clinical practice for monitoring the disease activity during treatment and for early detection of many infections, autoimmune, inflammatory, and malignant diseases.

Keywords: zinc oxide layer, surface-enhanced Raman spectroscopy (SERS), neopterin, atomic layer deposition (ALD)

1. Introduction

Surface-enhanced Raman scattering (SERS) is an optical spectroscopy method with high sensitivity and chemical specificity[1,2]. The phenomenon of SERS is explained by the combination of an electromagnetic (EM) mechanism and a chemical mechanism related to charge transfer (CT) between a substrate and an adsorbed molecule[3]. The electromagnetic enhancement results from the amplification of light by excitation of surface plasmon resonance (SPR) of the substrate. The chemical enhancement process involves the CT excitation between the frontier molecular orbitals a of the adsorbate and the Fermi level of the metal substrate. This excitation may occur if the excitation wavelength is resonant with the metal-molecule charge transfer electronic states. Of the two processes, the EM mechanism usually plays a larger role in SERS enhancement. Theoretically, the electromagnetic enhancement can reach factors of 10^3–10^{11}, whilst the chemical enhancement factors up to 10^3 were calculated[4,5]. The EM enhancement is associated with the "hot spots", which are spatially localized regions that exhibit extremely high field enhancement. Hot spots are created in the gap between two nanoparticles[6], but also near sharp edges, tips, and e.g., crossed nanowires[7]. It has been also proven that the SERS substrate with periodic structure leads to strong SERS enhancement[8].

Due to such large enhancement, even single molecules can be observed by SERS spectroscopy[9]. Additionally, the SERS technique offers nondestructive, reliable, and fast

detection of samples which leads to varied practical applications of this technique. SERS is powerful in studying nucleic acids and proteins[10], therapeutic agents[11], drugs and trace materials[12], microorganisms[13], and cells[14]. The most notable recent advances in SERS include innovative applications of bimolecular sensors for clinical diagnosis of various diseases, such as Alzheimer's or Parkinson's[15].

An ideal SERS substrate should exhibits a uniform and high enhancement factor (EF), chemical stability, and the possibility to be produced cheaply and reproducibly. Although considerable development has been made towards improving and optimizing SERS substrates, the standard application of SERS in biomedical and analytical tests is still hindered by the lack of effective SERS substrates which would satisfy all the requirements mentioned above. In recent years, many techniques have been used to prepare SERS substrates optimized in size, shape, and composition. These include electrochemical methods[16], nanosphere lithography[17], electron-beam lithography[18], nanoimprinting lithography[19] vapor layer deposition[20], and colloidal suspension[21].

In general, a classical SERS substrate is based on three metals, Au, Ag, and Cu, which have localized surface plasmon resonances in the visible and near infrared spectral regions. Recently, ZnO has been proposed as a promising candidate for fabrication of SERS-active substrates[22]. ZnO as a semiconductor: (i) offers high refractive index, which promotes strong light confinement leading to the increase of the SERS response[23], (ii) it may enhance the charge-transfer from the metal to the analyte and also contribute to improvement of the SERS effect[24]. Additionally, Sinha and co-workers[25] demonstrated the photocatalytic properties of ZnO (it is a wide band-gap material) to promote the UV -induced degradation of the analytes. This effect offers additional opportunities to clean up the SERS substrates for other measurements.

Usually, the ZnO nanorod and nanowire arrays are used as templates to fabricate silver or gold–coated nanocomposites for SERS measurements[26,27]. So far, these ZnO based SERS-active substrates were used only to test typical probe molecules such as *p*-mercaptobenzoic acid and Rhodamine 6G[28].

Many different fabrication techniques, such as hydrothermal methods, chemical vapor deposition or pulsed laser deposition have been used to synthesize ZnO nanostructures[29]. Among these various fabrication techniques of production of SERS substrates, atomic layer deposition (ALD) is used very rarely. Im et al.[30] used the ALD method as one of the three steps in the fabrication of Ag FON (Ag films over nanospheres), with a strong field enhancement inside 10 nm metallic nanogaps. In this approach the gap size was determined by the thickness of the Al_2O_3 layer, which can be precisely controlled by the number of ALD cycles.

We have developed novel SERS-active substrates based on Au coated ZnO layers prepared by the ALD method on a commercial silicon template. These substrates are based on ZnO films grown through a simple, self-limiting atomic layer deposition process. A thin (60 nm) layer of gold sputtered on the ZnO film provides activity to the obtained SERS platform.

The resultant SERS platforms show a very strong surface-enhancement factor (1×10^7), high stability (up to three months under ambient conditions), and high reproducibility, which could be used in the design of efficient SERS-active platforms for analytical applications. These Si/ZnO/Au substrates exhibit good performance toward sensitive and reproducible SERS-based detection of neopterin. In this study we show, for the first time, the possibility of quantitative SERS analysis of this marker for cellular immune system activation in human blood plasma.

Neopterin, a pyrazonopyrimidine compound is synthesized from guanosine triphosphate by human monocytes and macrophages after stimulation by interferon gamma (IFN-γ) derived

from antigen-activated T lymphocytes[31]. It is formed by GTP cyclohydrolase I that converts GTP into 7,8-dihydroneopterin triphosphate, which is in the next step metabolized to neopterin.[32] Determination of neopterin indicates the state of activation of the cellular immune system during subsequent stages of various diseases, such HIV-1[33] (Human immunodeficiency virus type 1) or rheumatoid arthritis[34]. The high level of neopterin is also associated with viral (hepatitis A, B, and C, Cytomegalo, measles, rubella, influenza) and bacterial infections[35], cardiovascular disease[36], insulin resistance[37], and some tumors[38]. Up to now several analytical procedures evaluated the level of neopterin in blood using mainly high pressure liquid chromatography (HPLC)[39] and enzyme-linked immunosorbent assay (ELISA)[40] measurements. However, both of these methods are time-consuming and expensive; they also require complex technical equipment and highly trained personnel. Over the last decade, SERS has turned out to be promising in bimolecular sensing for clinical diagnosis. In this work we present a possibility of using SERS spectroscopy for quantitative detection of serum neopterin level. It should be highlighted that the elevated neopterin levels in body fluids were found at the end of the incubation period before the beginning of clinical symptoms. Therefore, such method as SERS, which allows monitoring the neopterin level even before the specific antibodies against the virus become detectable, is particularly useful. Neopterin level detection based on SERS measurements might be a unique method to evaluate the protective efficiency of vaccines stimulating cell-mediated immunity against viral, bacterial, and parasitic diseases. Additionally, SERS has unique advantages for rapid label–free detection of analytes because of high sensitivity, selectivity, elimination of expensive reagent and time-consuming sample preparations.

2. Experimental section

2.1. Chemicals and materials

Neopterin (D-erythro-1', 2', 3'-trihydroxypropylpterin) was obtained from Tocris Bioscience (Bristol, UK). *p*-MBA (*p*-mercaptobenzoic acid) and phosphate-buffered saline (PBS) packs (10 mM, pH = 7.2) from Sigma-Aldrich (Dorset, UK). were used without further purification. Water (resistivity over 18 MU), purified using a Milli-Q plus 185 system was used throughout the process. In our experiments we used human blood samples from 8 healthy volunteers available by courtesy of Regional Blood Center. The samples underwent morphological analyses prior to use and revealed no abnormalities. All plasma and serum samples were evaluated for neopterin by using the commercial enzyme-linked immunoassay test (ELISA, IBL International GmbH, Hamburg) in order to determine the output concentration of neopterin in studied samples. For ZnO deposition commercial 300 μm thick Si (100) wafers from El-Cat Inc. (USA) were used.

2.2. Instrumentation

2.2. Instrumentation

Raman and SERS Spectroscopy measurements were carried out with a Renishaw inVia Raman system equipped with a 785 nm diode laser. The light from the laser was passed through a line filter and focused on a sample mounted on an X–Y–Z translation stage with a 20× microscope objective, NA = 0.25. The beam diameter was approximately 5 μm. The laser power at the sample was 5mW or less. The microscope was equipped with 1200 grooves per mm grating, cutoff optical filters, and a 1024 x 256 pixel Peltier-cooled RenCam CCD detector, which allowed registering the Stokes part of Raman spectra with 5–6 cm^{-1} spectral

resolution and 2 cm^{-1} wavenumber accuracy. The experiments were performed at ambient conditions using a back-scattering geometry.

Collecting of SERS spectra

For the recording of spectra, the SERS platform was placed into a chamber of 15µl volume fabricated in polycarbonate. A 10µl volume of the analyte solution was applied with a microliter syringe. The recording of the spectra started immediately after placing this chamber under the microscope lens. During the period of at least 10min, SERS spectra were repeatedly recorded; at the same time, the focus of the laser beam was readjusted. The time required for completing a single SERS spectrum was about 40s.

The obtained spectra were processed with the Wire3 software provided by Renishaw. Some of the spectra required post processing, involving spike removal and six-point baseline correction. Smoothing of the spectra was not employed.

PXRD (powder X-ray diffraction spectroscopy) data were collected using the PANalytical Empyrean diffractometer. Measurements employed Ni-filtered Cu Kα radiation of a copper sealed tube charged with a 40 kV voltage and a 40 mA current in a Bragg-Brentano geometry with beam divergence of 1/4 deg. in the scattering plane. Diffraction patterns were measured in the range of 5 - 140 degrees of the scattering angle by step scanning with a step of 0.01 degree.

SEM measurements were performed under high vacuum using the FEI Nova NanoSEM 450 with an accelerating voltage of 10 kV under high vacuum.

2.3. SERS substrate preparation

ZnO film preparation

Zinc oxide films were deposited on Si(100) substrates by Atomic Layer Deposition at 100^{o}C. The ALD technique is a growth method similar to chemical vapor deposition (CVD). The main difference is a sequential deposition procedure of the ALD process in which two reagents (called "precursors") are alternatively introduced into the growth chamber. This results in a self-limiting chemical reaction occurring only at the surface of the growing film. Because of this the ALD growth provides conformal and uniform films with reproducible thickness.

In the present study we used diethylzinc (DEZn) as a zinc precursor and deionized water as an oxygen precursor. High purity nitrogen was applied as purging gas. Zinc oxide has been created as a result of a double-exchange chemical reaction that takes place at the surface:

$$Zn(C_2H_5)_2 + H_2O \rightarrow ZnO + 2C_2H_6$$

The growth process was performed in the Savannah-100 reactor. Both precursors, diethylzinc and water, were kept at room temperature. Before the ALD growth, silicon wafer was rinsed out in trichloroethylene, acetone, and isopropanol and then cleaned in deionized water. The ZnO films used in the present study were grown with 10000 ALD cycles, which resulted in the film thickness of 1.4 μm.

Procedure of gold sputtering: to sputter a layer of gold we used the PVD equipment from Leica, model EM MED020. The gold target was obtained from Mennica Metale Szlachetne, Warsaw, Poland. The size of the target was 54 mm in diameter, 0.5 mm thickness and gold

purity was 5N. The vacuum during the gold sputtering was on the level of 10^{-2} mbar. The sputtering current was 25 mA. After the deposition process the samples were placed into a sterile Petri dish. Three different thicknesses of gold (30, 80, and 160 nm) were tested to find optimal conditions for SERS enhancement. The 30 nm gold layer was not sufficiently thick to obtain the appropriate SERS signal of the analyte (*p*-MBA and neopterin). In the case of ZnO layer covered with 80 nm of gold we observed the highest SERS enhancement without any signals from ZnO. We achieved the same level of enhancement for 160 nm gold layer. For further experiments we chose 80 nm thick layer of gold.

3. Results and discussion.

3.1. Characterization of Si/ZnO/Au surface

Structure and surface morphology of zinc oxide films grown by ALD strongly depend on such parameters of the growth process as temperature and purging time[41]. For the present study we chose low deposition temperature (100^{o}C) and short purging time (2s), which result in developed surface morphology. Root Mean Square (RMS) of the surface roughness of the ZnO film without Au coating was measured by Atomic Force Microscopy (AFM) for ZnO films with different thickness. It was found that for 630 nm thick ZnO layer RMS value is 24 nm, while for 1 µm thick ZnO layer the RMS is 38.5 nm, and for the 1.4 µm thick ZnO films the RMS value is 68 nm. The measured EF values for the above films are 3.3 x 10^2, 1.4 x 10^6 and 4.2 x 10^7, respectively. The 1.4 µm thick ZnO layer was chosen for further studies, as it shows the best EF characteristic. In Fig. 1 we show the lateral view of the ZnO surface (left) and the exemplary cross-section across the surface. The scale in Fig. 1(right) is given in nm. One can see that the difference between the minimum and the maximum height is about 400

nm and considerably exceeds the RMS value which is an arithmetic average. It can be noticed that despite a high roughness the ZnO surface is very homogeneous.

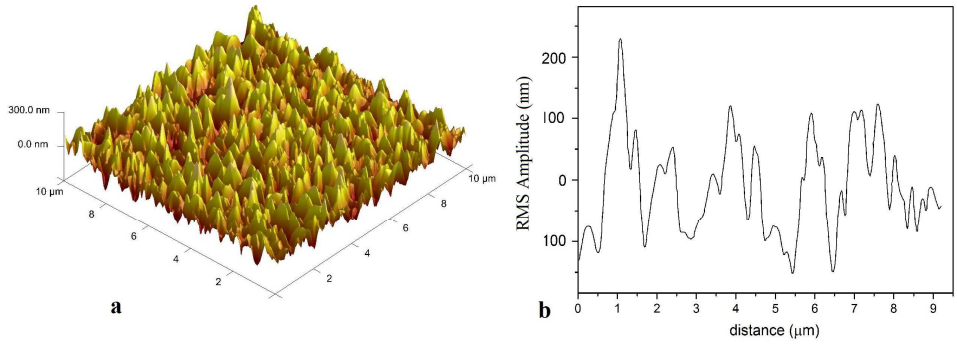

Fig. 1. (a) The AFM image of the ZnO film used as a SERS platform, (b) The exemplary cross-section of the surface of the ZnO film.

Figure 2 shows the representative SEM image of Au–coated Si/ZnO films at different magnifications. The close examination of the SEM images reveals that the diameter of gold semi-spheres is about 40 – 60 nm

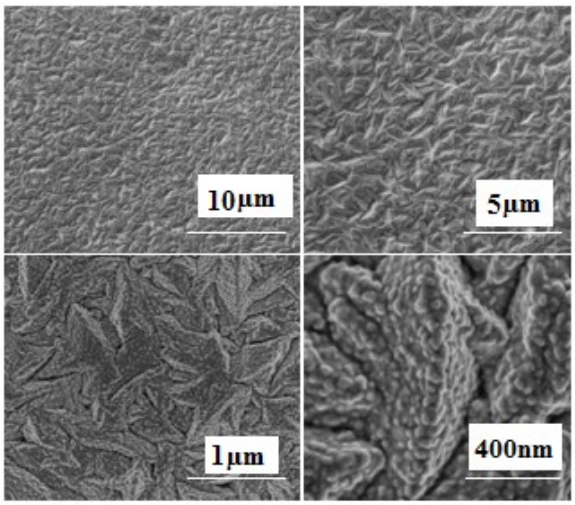

Fig. 2. SEM images of Au–coated Si/ZnO films at different magnifications.

Additionally, PXRD (powder X-ray diffraction spectroscopy) analysis was employed to investigate the crystal phase of Si/ZnO and Si/Zn/Au (see the Supporting Information, Fig. S1). The crystal structure of both, the ZnO layers and Au sputtered onto ZnO were characterized by XRD (PANalytical X'Pert Pro X-ray diffractometer) with Cu Kα radiation (λ = 0.15418 nm). Figure S1shows XRD patterns of the ZnO layer without Au coating. The peaks at 2θ = 31.58°, 34.46°, 36.26°, 56.74°, 61.73° were assigned to (100), (002), (101), (110), (103), indicating the hexagonal wurtzite structure of ZnO. For Au/ZnO/Si films we registered a gold signal and no signal from the ZnO, concluding that the layer of gold on the Si/ZnO array is uniform and all SERS signals come from molecules localized on the surface of gold.

3.2. SERS properties of Si/ZnO/Au substrate

In order to examine the SERS activity of the ZnO/Au substrate, we calculated the enhancement factors; *p*-MBA was chosen as a standard analyte. The obtained normal Raman and SERS spectra are depicted in Fig. S2. The ZnO/Au substrate was incubated in 9.0 mL of 1.0×10^{-6} M *p*-MBA solution in water for 60 min and then washed with deionized water. The Raman bands at 715, 843, 100, 1079, 1374 and 1593cm^{-1}are typical for *p*-MBA[42], and can be treated as a fingerprint of this molecule. Table S1 summarizes band assignments for the normal Raman spectrum of *p*-MBA and its SERS spectrum. The surface enhancement factor (EF) for *p*-MBA was calculated according to the following equation:

$$EF = \frac{I_{SERS} N_{NR}}{I_{NR} N_{SERS}} \quad (1)$$

where N_{SERS} and N_{NR} refer to the number of molecules adsorbed on the SERS probe within the laser spot area and the number of molecules probed by regular Raman spectroscopy, respectively. I_{SERS} and I_{NR} correspond to the SERS intensity of *p*-MBA on the modified

surface and to the normal Raman scattering intensity of *p*-MBA in the bulk. I_{NR} and I_{SERS} were measured at 1079 cm^{-1}.

The crucial parameters for the quantitative analysis of the spectra are the laser spot area and the effective illuminated volume. The latter has been estimated using a formula recommended by Renishaw:

$$V = 3.21 \times \lambda^3(f/D) \quad (2)$$

where f is the microscope objective focal length and D denotes the effective laser beam diameter at the objective back aperture. For our setup, $V = 2012 \approx 2\times10^3$ μm^3. The laser beam diameter, defined as twice the radius of a circle encompassing the area with 86% of the total power was about 5 μm; approximately the same values were obtained from the experimentally obtained laser spot image and from the theoretical formula ($4\lambda f/\pi D$). Assuming the volume in a shape of a cylinder with the diameter of 5 μm leads to the effective height of 100 μm. This value was confirmed by recording Raman spectra of Si while varying the distance from the focal plane. The SERS samples were prepared by dipping the substrate in 9.0 mL of 1.0×10^{-6} M solution of *p*-MBA. The number of molecules contained in the solution was 5.4×10^{15} ($6{,}02 \times 10^{23}$ molecules/mol $\times$ 9.0 $\times 10^{-3}$ L $\times$ 1.0×10^{-6} mol/L = 5.4×10^{15} molecules). The surface area irradiated by the laser beam (5 μm in diameter) was 19.6 μm^2 (3.14 $\times$ (2.5 μm^2) = 19.6μm^2). The surface of our samples was 20 mm^2. Therefore, about 4.2×10^9 molecules were present in the laser beam spot. The normal Raman spectrum was observed for a cell filled with a pure *p*-MBA acid (154.19 g/mol; density of 1.06 g/cm^3). The effective illuminated volume for our setup is 2×10^3 μm^3. Under these conditions, $N_{NR} = 8.1 \times 10^{12}$ molecules were irradiated by the laser.

From these data of the relative intensity and the number of molecules sampled from the regular Raman and SERS measurements, the enhancement factor was calculated to be about 4.2 x 10^7. The achieved level of enhancement makes this method of SERS platform fabrication a promising strategy for practical SERS applications.

SERS efficiency depends on surface morphology. We used three different ALD procedures to obtain various thicknesses of ZnO layers: 1 μm; 1.4 μm and 630 nm. SERS spectra of *p*-MBA molecules cast from 10^{-6} M aqueous solution onto these three surfaces have been recorded and presented in Figure S3. Also, the enhancement factor for each surface was calculated using eqn (1) and presented in Table S2. The optimal thickness of ZnO layers (1.4 μm) corresponded to highest roughness of the surface (RMS value in Table S2) and to the highest EF (Table S2).

3.3. Stability and reproducibility of the SERS substrate

The reproducibility of recorded signals is one of the crucial parameter for bio-analytical and medical analysis. To verify the signal reproducibility of our substrate, SERS spectra of *p*-MBa molecules (10^{-9} M solution in water) from randomly 50 selected places on a Si/ZnO/Au substrate were collected under the same experimental conditions. As can be seen in Fig. 3, the Si/ZnO/Au substrate exhibits very good SERS sensitivity and reproducibility. The Raman spectra of *p*-MBa are enhanced strongly at each acquisition point. To get statistically meaningful results, the strong band at 1079 cm^{-1} was chosen to calculate the relative standard deviation (RSD). The RSD of the intensity of these Raman vibrations in the 50 SERS spectra collected on the same platform (area of 0.5 × 0.5 cm) is 9 %. The reproducibility of the SERS signals recorded from different samples prepared using the same method was also tested. We collected 20 spectra from 20 different (separately fabricated) SERS platforms. The achieved

RSD was 11%, which clearly indicates that the prepared SERS substrate can be considered as a highly reproducible SERS platform. The obtained RSD value for our substrates is comparable to the RSD value of a commercial substrate Klarite (RSD = 14%).

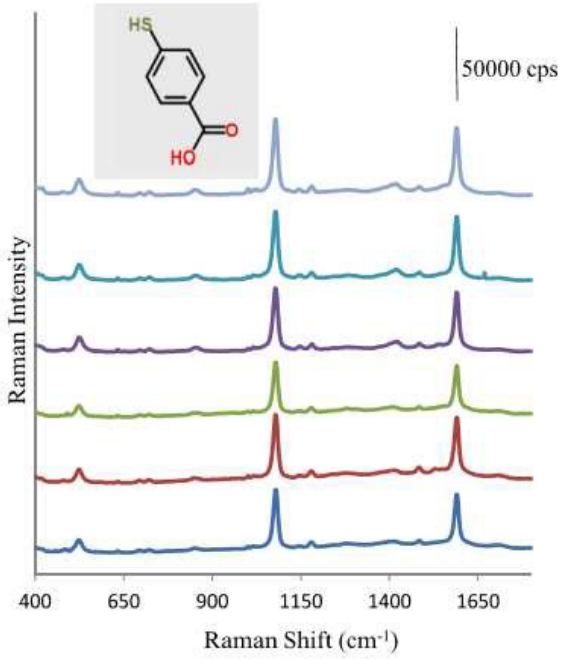

Figure 3. The representative SERS spectra of *p*-MBA recorded from 50 different spots on the SERS surface. Experimental conditions: 5mW of 785 nm excitation, 4 x 10 seconds acquisition time. Each SERS spectrum was averaged from seven measurements taken at different spots of the SERS surface. The *p*-MBA spectra have been baseline- corrected and shifted vertically for better visualization.

The stability of a SERS substrate determines the range of its practical applications in chemical and biological analysis. The crucial parameters are the stability against oxidation for an extended period of time. Figure 4 illustrates the SERS spectra of *p*-MBA recorded on a freshly prepared Si/ZnO/Au surface (Fig. 4a) and on a surface exposed to air for 3 months. Considering the 1079 cm^{-1} band as a reference, the intensity of *p*-MBA was reduced approximately by only 3% after three months of storing the surface under atmospheric

conditions (Fig.4b). Such high stability and reproducibility enables the quantitative SERS studies of numerous biomolecules and improves the SERS potential in real applications.

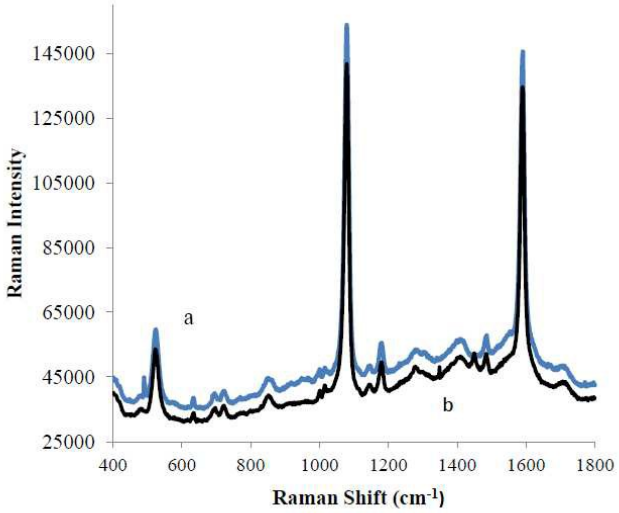

Figure 4. SERS spectra of *p*-MBA recorded on (a) freshly prepared Si/ZnO/Au surface and (b) on a Si/ZnO/Au surface stored for three months under ambient conditions. Experimental conditions: 5mW of 785 nm excitation, 4 x 10 seconds acquisition time. Each SERS spectrum was averaged from 15 measurements at different places across the SERS surface.

3.4. Detection of Neopterin in blood plasma sample

Neopterin is a small molecule which is biologically and chemically stable in body fluids, gives strong SERS signals and therefore can be applied for label–free measurements in the laboratory using the Raman technique[43]. Neopterin appears in both human blood (plasma, serum) and urine, and its increased levels show an activation of the immune system involved in the pathogenesis and/or affected by malignant diseases. An earlier literature report[44] reveals that Raman spectroscopic characterization of urine allows to identify the biomarkers such as neopterin for early detection of oral cancer. In this study we show the possibility of SERS detection of neopterin in human blood plasma. Figure 5 presents the normal Raman spectrum

of neopterin (Fig. 5 insert) and the concentration-dependent SERS spectra of neopterin in PBS buffer (Fig.5 a-g)

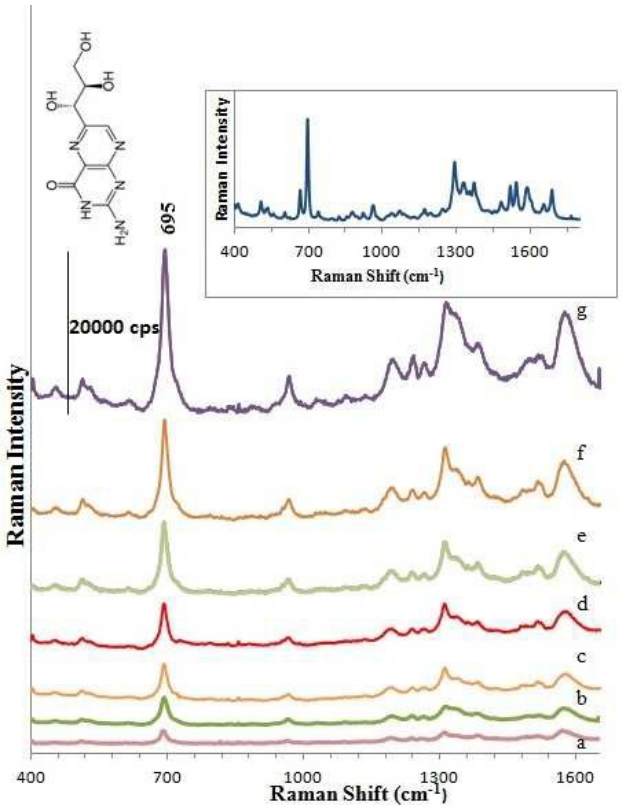

Figure 5. SERS spectra obtained for increasing concentration of neopterin: (a) 3.0; (b) 5.0; (c) 7.0; (d) 10.0; (e) 20.0; (f) 45.0; and (g) 150.0 nmol/L in a PBS buffer solution. The insert shows the normal Raman spectrum of neopterin powder. Experimental conditions: 5mW of 785 nm excitation, 4 x 10 seconds acquisition time. The SERS spectra have been baseline-corrected and shifted vertically for better visualization. Each SERS spectrum was averaged from seven measurements from different places of the SERS platform. Normal Raman spectrum of neopterin powder was obtained with 5 accumulations of 30s each, using 50mW of 785 nm excitation.

As can be seen, the normal Raman signal of neopterin powder is dominated by bands at 668, 698, 963, 1293, 1519, 1544, 1583 and 1688 cm^{-1}. Most of the bands present in the

normal Raman spectrum appear in the SERS spectrum of neopterin after adsorption onto Si/ZnO/Au substrate. Some bands undergo a small shift in position upon adsorption onto the SERS surface. The SERS spectra of neopterin (Figure 5 a-g) are dominated by bands at 695, 1308, 1578 and 1690 cm^{-1} and due to C-C vibration and ring modes, N–H bending modes, NH_2 symmetric deformation, and C=O stretching vibrations, respectively[45].

In order to test the performance of our SERS surface in terms of sensitivity and low detection limit (LOD), the plot of SERS intensity of the marker band at 695 cm^{-1} versus the concentration of neopterin in PBS buffer was constructed (Fig. 6).

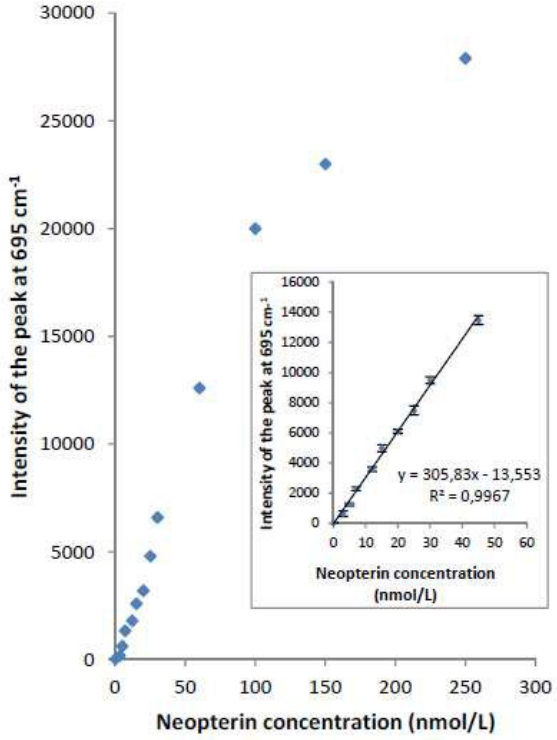

Fig. 6**.** The relationship between the intensity of the band at 695cm^{-1} versus the concentration of neopterin in buffer solution in the range from 0 to 250 nmol/L. The inserted figure shows the plot of the intensity of this band versus the concentration of neopterin in the range from 0 to 40 nmol/L. Experimental conditions: 5mW of 785 nm excitation, 4 x 10

seconds acquisition time. Each SERS spectrum was averaged from seven measurements from different places of the SERS platform.

A dilution series was created using concentrations of 0.0, 3.0, 7.0, 10.0, 20.0, 25.0, 30.0, 60.0, 100.0, 150.0, and 250.0 nmol/L. The intensity of the marker band increases linearly with increasing concentration of neopterin and demonstrates the potential of our label-free SERS detection method for the quantitative determination of neopterin levels in real blood samples. Figure 6 shows the relationship between the intensity of band at 695 cm^{-1} versus the concentration of neopterin over the whole tested concentration range. The insert in Figure 6 illustrates a calibration curve obtained by plotting the intensity of this marker band versus the concentration of the neopterin in the range from 0.0 to 40.0 nmol/L. The error bars indicate the standard deviations from seven measurements of different spots for each concentration. In the linear region the calibration curve was fitted as $y = 305.83x + 13.553$ and the correlation coefficient (R^2) was 0.997. For the linear calibration curve, it was assumed that the SERS intensity at 695 cm^{-1} (y) is linearly related to the concentration of neopterin (x). Additionally, the low detection limit (LOD) was estimated using the signal-to-noise method.[46] The results gave the LOD = 1.1 nmol/L which is comparable to commercially available ELISA test (LOD = 0.8 nmol/L)[47]. The above results indicate that the developed Si/ZnO/Au substrate is ideal for biomarker detection in human body fluids. Hence, in the next step, this SERS substrate was evaluated for detecting neopterin in the human blood plasma. The samples of neopterin in human blood plasma with different concentrations, reflecting clinically relevant neopterin titers, (3 – 250 nmol/L) were prepared. Blood plasma was separated from the blood by centrifugation at 3000 rpm for 15 min. In order to find the output concentration of neopterin in studied blood plasma, all samples were evaluated for neopterin by using the commercial enzyme-linked immunoassay test (ELISA, IBL International). For

each of the eight healthy unvaccinated volunteers the level of neopterin was 4.2 nmol/L. The value < 5 nmol/L is as a typical concentration of plasma neopterin in nonimmune patients[48]. For comparison, in patients in early stages of HIV-infection the extremely high neopterin levels in serum (at about 100 nmol/L) were detected[49]. In clinical practice the presence of neopterin is monitored in whole blood, serum, plasma or cerebrospinal fluid.

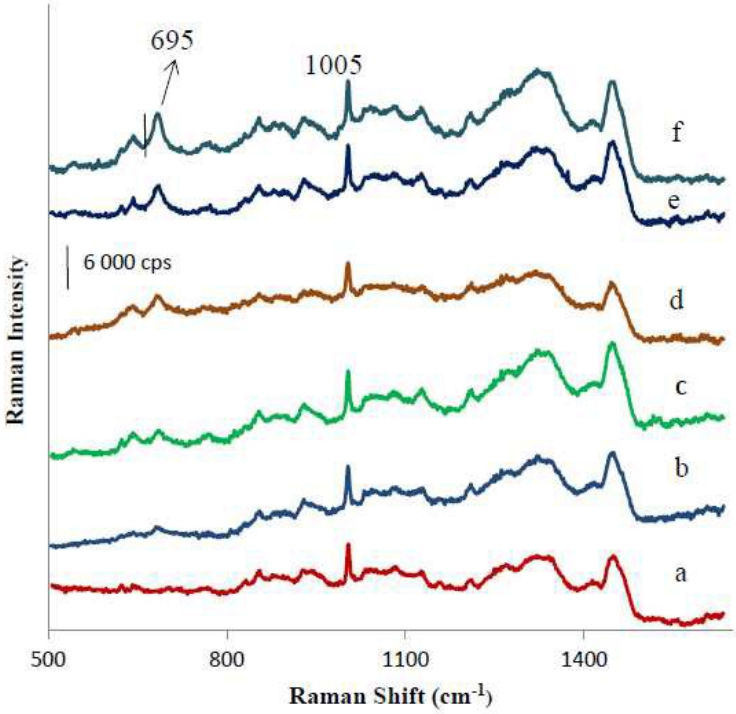

Figure 7. SERS spectra of human blood plasma (a); b-f, the SERS spectra obtained for increasing concentration of neopterin in human blood plasma: (b) 5.0; (c) 7.0; (d) 10.0; (e) 50.0, and (f) 150.0 nmol/L. Experimental conditions: 5mW of 785 nm excitation, 4 x 20 seconds acquisition time. The SERS spectra have been baseline corrected and shifted vertically for better visualization. Each SERS spectrum was averaged from seven measurements in different places of SERS platform.

Figure 7 b-f shows the selected SERS spectra recorded in the presence of different concentration of neopterin in blood plasma. Figure 7a presents the SERS spectrum from a

"pure human blood plasma" (without adding neopterin) placed onto the Si/ZnO/Au surface. The SERS spectra were acquired "in situ " from the SERS–surface placed in plasma solution. In the range of 350 – 1750 cm^{-1} the SERS spectrum of blood plasma is dominated by a number of bands (652, 1021, 1141, 1233, 1265, 1343, 1588, and 1665 cm^{-1}) arising from proteins, amino and nucleic acid, and lipids[50]. Although this SERS spectrum is complex and provides a rich source of information about numerous blood components, the region of blood plasma (660-720cm^{-1}), in which the marker band of neopterin should appear (695cm^{-1}), is signal-free and allows label-free analysis of neopterin. Moreover, in order to obtain better diagnostic accuracy, a simple algorithm based on the empirical analysis of Raman spectra[51] in terms of the peak intensity ratio was employed. The ratio of intensities at 695cm^{-1} (neopterin marker) and 1005 cm^{-1} (phenylalanine marker in plasma) was used to estimate the concentration of neopterin in blood plasma. Other bands of neopterin at 1293 and 1580cm^{-1} show very weak intensity and appear in the SERS spectrum as a shoulder on the bands corresponding to human plasma. Only for patients with Phenylketonuria (genetic disease) the peak of phenylalanine cannot be considered as the internal standard because the plasma phenylalanine level is not stable and range from 6 to 80 mg/dL depending on dietary treatment[52]. Then to establish relationship between the intensity bands versus the concentration of neopterin only the intensity at 695 cm^{-1} (neopterin marker) should be taken into account.

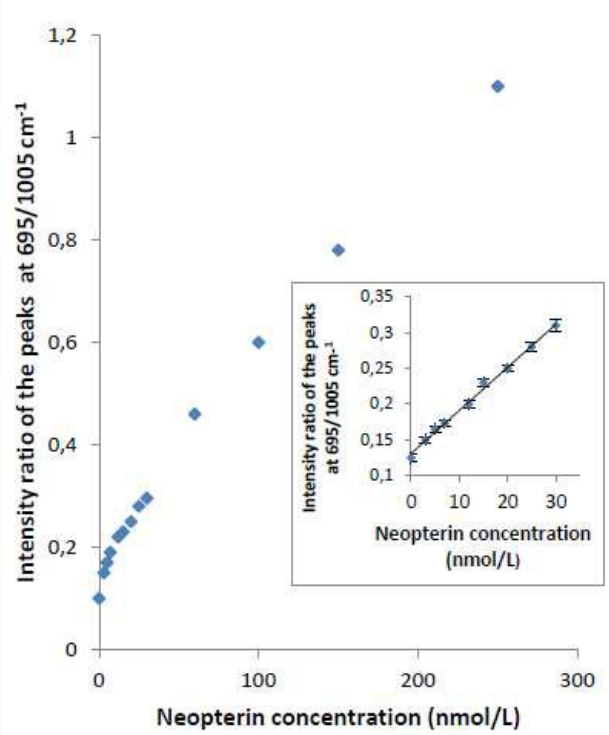

Figure 8. The relationship between the intensity ratio of 695/1005 cm^{-1} bands versus the concentration of neopterin in blood plasma in the range from 0 to 250 nmol/L. The inserted figure shows the plot of this intensity ratio marker band versus the concentration of neopterin in the range from 0 to 30 nmol/L. Experimental conditions: 5mW of 785 nm excitation, 4 x 20 seconds acquisition time. Each intensity of SERS spectrum was averaged from seven measurements in different places of SERS platform.

Figure 8 shows the plot of the intensity ratio of 695/1005 cm^{-1} SERS bands as a function of neopterin concentration in blood plasma. The intensity ratio of SERS peaks rises with the increase in the concentration of neopterin in plasma. The LOD for neopterin was estimated using the signal-to-noise method mentioned above. The results show that LO is as low as 1.4 nmol/L, which reflects the potential of label-free SERS method and the developed Si/ZnO/Au-SERS–surface for biomarkers detection in real body fluids. The lower current

limit for a detection specification for the commercial ELISA test ranges from 0.7 to 2.2 nmol/L.

The reproducibility of the presented SERS label-free strategy towards neopterin detection was also investigated. Figure S4 shows 15 individual readings from 1 to 15 randomly selected spots for three different Si/ZnO/Au surfaces immersed in buffer solutions with different concentrations of neopterin (5.0, 10.0, and 25.0 nmol/L). To get a statistically valid result, the marker band of Raman reporter at 695 cm^{-1} was chosen to calculate the relative standard deviation (RSD). The corresponding relative standard deviations were 10.0, 11.0, and 8%, respectively. The relative average standard deviation (RSD) of this method is less than 10%, which is comparable to that of conventional ELISA assays.

Moreover, our approach offers a rapid, sensitive, high-throughput, suitable for point-of-care and innovative low-cost analysis to monitor diseases associated with the activation of cell-mediated immunity. This study will be extended in the future to detection of neopterin in real clinical blood plasma samples.

Conclusions

The present study demonstrates that atomic layer deposited zinc oxide films on silicon wafers are of great potential for efficient fabrication of SERS-active substrates. Our experimental results indicate that this SERS-active substrate with its strong surface-enhancement factor, high stability and reproducibility can be used for label–free SERS detection in both, biological and non-biological samples. For *p*-mercaptobenzoic acid the enhancement factor (EF) of the Raman signal on a Si/ZnO/A-surface was estimated as 10^7. The SERS measurement reflect the excellent reproducibly of these substrates, both between platforms and across the single platform. The quantitative SERS–based detection of neopterin over a

broad, clinically relevant concentration range (0 - 250 nmol/L) was demonstrated for the first time. The detection limit, in blood plasma, for neopterin on the Si/ZnO/Au-SERS surface was found to be 1.4 nmol/L. This study will be extended in future to neopterin detection in clinical blood plasma samples of patients with specific infections. Determination of neopterin levels might be also used in the future for more accurate evaluation of diseases and hence upcoming prognosis.

Acknowledgements

The research was supported by the European Union within European Regional Development Fund, through Innovative Economy grant (POIG.01.01.02-00-008/08). AK acknowledges the support from NCBiR under grant PBS2/A1/8/2013.

References

[1] S. Nie, S.R. Emory, *Science*, 1997, **257**, 1102.

[2] Y. Wang, L. Chen, *Chemical Reviews*, 2013, **3**, 1391.

[3] A. Campion and P. Kambhampati, *Chem. Soc. Rev.*, 1998, **27**, 241.

[4] P. L. Stiles, *Ann. Rev. Anal. Chem.*, 2008, **1**, 601.

[5] J. P. Camden, *J. Am. Chem. Soc*., 2008, **130**, 12616.

[6] M. Li, S.K. Cushing, J. Zhang, J. Lankford, Z.P. Aguilar, D. Ma, N. Wu, *Nanotechnology*, 2012, **23**, 115501.

[7] G. Braun, I. Pavel, A.R. Morrill, D.S. Seferos, G.C. Bazan, N.O. Reich, M. Moskovits ; *J. Am. Chem. Soc*., 2007, **129**, 7760.

[8] M. Li, S. K. Cushing, H. Liang, S. Suri, D.Ma, N. Wu, *ACS Nano*, 2011, **5**, 9082.

[9] E.C. Le Ru, P. G. Etchegoin, *Annu .Rev. Phys. Chem*., 2012, **3,** 1437.

[10] K. Kneipp. H. Kneipp, V.B. Kartha, R. Manoharan, G. Deinum, I. Itzkan, R.R. Dasari, and M.S. Feld, *Phys. Rev. E*, 1998, **57**, R6281.

[11] R.S. Stokes, E. McBride, C.G. Wilson, J.M. Girkin, W.E. Smith and D. Graham, *Appl. Spectrosc.*, 2008, **62**, 371.

[12] K. Faulds, W.E. Shmith, D. Graham and R.J. Lacey, *Analyst*, 2002, **127**, 282.

[13] A. Sivanesan, E. Witkowska, W. Adamkiewicz, Ł. Dziewit, A. Kamińska, J. Waluk, *Analyst* 2014, **139**,1037.

[14] T.A. Alexander and D.M. Le, *Appl. Opt.*, 2001,**46**,3878.

[15] H.T. Beier, *Plasmonics*, 2007, **2**, 55

[16] H.H. Wang, C.Y. Liu, S.B. Wu, N.W. Liu, C.Y. Peng, T.H. Chan, Ch.F. Hsu, J.K. Wang, Y. L. Wang, *Adv.Mater*., 2006, **18**, 491.

[17] L.A. Dick, A.D. McFarland, C.L. Haynes and R.P. Van Duyne, *J. Phys. Chem.B*, 2002, **106**, 853.

[18] D.P. Fromm, A. Sundaramurthy, A. Kinkhabwala, P.J. Schuk, F.S. Kino and W.E. Morner, *J. Chem. Phys.,* 2006, **124**, 01101.

[19] R. Alvarez-Puebla, B. Cui, J.-P. Bravo-Vasqurez, T. Veres and H. Fenniri., *J. Phys. Chem. C*, 2007, **111**, 6720.

[20] D.J. Semin, K.L. Rowlen, *Anal. Chem.,* 1994, **66**, 4324.

[21] K. Faulds, W.E. Shmith, and D. Graham, *Anal.Chem.*, 2004, **76**, 412.

[22] C. Cheng, B. Yan, S.M. Wong, H. Li, W. Zhou, T.Yu, Z.Shen, H.Yu, H.J. Fan., *Applied Materials and Interfaces,* 2010, **2**, 1824.

[23] H. Qi, D. Alexon, O. Glembocki, S. Prokes, *Nanotechnology*, 2010, **21**, 085705.

[24] L. Yang, W,Ruan, X.Jiang, J.R. Lombardi, *J. Phys. Chem. C*, 2009, **113**, 117.

[25] G. Sinha, L.E. Depero, I. Alessandri, *Applied Materials and Interfaces*, 2011, **3**, 2557.

[26] L.M. Chen, L.B. Luo, Z.H. Chen, M.L. Zhang, J.A. Zapien, C.S. Lee and S.T. Lee, J. *Phys. Chem. C*, 2010, **114**, 93.

[27] L. Sun, D. Zhao, Z. Zhang, B. Li, D. Shen, *Journal of Material Chemistry*, 2011, **21**, 9674.

[28] A.E. Kandjani, M. Mohammadtaheri, A. Thakkar, S.K. Bhargava, V. Bansal*, J. Colloid. and Interface Science*, 2014, **436**, 251.

[29] C. Li, G. Fang, F. Su, G. Li, X. Wu, X. Zhao, *Nanotechnology,* 2006, **17**, 3740.

[30] H. Im, K.C. Banz, S.H. Kee, T.W. Johnson, C.L. Haynes, S.H. Oh, *Adv. Materi.*, 2013, **25**, 2678.

[31] C. Huber, J.R. Batchelor, D. Fuchs, A. Hausen, A. Lang, D. Niederwieser, G. Reibnegger, P. Swetly, J. Troppmair and H. Wachter., *Journal of Experimental Medicine,* 1984, **160**, 310.

[32] C. Murr, B. Widner, B. Wirleitner, D. Fuchs, *Curr Drug Metab*, 2002, **3**, 175.

[33] Wirleitner B, K. Schroecksnadel , C. Winkler , D. Fuchs, *Mol. Immunol.*, 2005, **42**, 183.

[34] D. Arshadi, B. Nikbin, Y. Shakiba, A. Kiani, A.R. Jamshidi, M.T. Boroushaki, *International Immunopharmacology*, 2013, **17,** 763.

[35] D. Fuchs, A. Hausen, M. Kofler, H. Kosanowski, G. Reibnegger and H. Wachter, *Lung* 1984, **162**, 337.

[36] X. Garcia-Moll, D. Cole, E. Zouridakis and JC. Kaski, *Heart,* 2000, **83**, 346.

[37] M. Ledochowski, C. Murr, B. Widner and D. Fuchs, *Clinical Chimica Acta ,* 1999, **282**, 115.

[38] C. Murr, A. Bergant, M. Widschwendter, K. Heim, H. Schrocksnadel and D. Fuchs, *Clinical Chemistry,* 1999, **45**, 1998.

[39] E.R. Werner, A. Bichler, G. Daxenbichler, D. Fuchs, L.C. Fuith, A. Hausen, H. Hetzel, G. Reibnegger and H. Wachter, *Clinical Chemistry,* 1987, **33**, 62.

[40] M. Barak, D. Merzbach and N. Gruener, *Scandinavian Journal of Clinical Laboratory Investigations,* 1990, **50**, 705.

[41] I.A. Kowalik, E. Guziewicz, K. Kopalko, S. Yatsunenko, A. Wójcik-Głodowska, M. Godlewski, P. Dłużewski, E. Łusakowska, W. Paszkowicz, *J. Cryst. Growth,* 2009, **311**, 1096.

[42] A. Michota and J. Bukowska, *J. Raman Spectrosc.,* 2003, **34**, 21.

[43] E.R. Werner, A. Bichler, G. Daxenbichler, *Clin Chem.,*1987, **33,** 62.

[44] B. Elumalai, A. Prakasarao, B. Ganesan, K. Dornadula, S. Ganesan, *J. Raman Spectrosc.*, 2015, **46**, 84.

[45] N. Prabavathi, A. Nilufer, V. Krishnakumar, *Spectrochimica Acta Part A*, 2013,**114**, 101.

[46] A. Shrivastava, V.B. Gupta, *Chron Young Sci. ,* 2011, **2**, 21.

[47] M. Bayer, S. Schmitz, J. Westermann, F. Thiemann, R. Edelmann, C. Szakacs, G. Lanzer, J. Blecken, *Clin Lab.*, 2005, **51**, 495.

[48] L. Hagberg, L. Dotevall, G. Norkrans, H. Wachter, D. Fuchs, *J Infect Dis* , 1993, **168**, 1285.

[49] J.L. Fahey, J.M.G. Taylor, R. Detels, B. Hofmann, R. Melmed, P. Nishanian and J.V. Giorgi, *New Engl J Med.*, 1990, **322**, 166.

[50] W.R. Premasiri, J.C. Lee, L.D. Ziegler, *J. Phys. Chem B.,* 2012, **116**, 9376.

[51] D. Lin, S. Feng, J. Pan, Y. Chen, J. Lin, G.Chen, S. Xie, H. Zeng, R. Chen, *Opt.Express*, 2011, **19**, 133565.

[52] U. Langenbeck, J. Zschocke, U. Wendel, V. Hönig, *J. Inherit. Metab. Dis.,* 2001, **8**, 805.